Supporting Information

Polyoxometalates /Active Carbon Thin Separator for Improving Cycle Performance of Lithium-Sulfur Batteries

Wei Yao, Li Liu, Xuesong Wu, Chao Qin,* Haiming Xie, and Zhongmin Su*

National & Local United Engineering Laboratory for Power Battery, Key Laboratory of Polyoxometalate Science, Institute of Functional Material Chemistry, Northeast Normal University, Changchun, Jilin, 130024, P. R. China

*E-mail: qinc703@nenu.edu.cn and zmsu@nenu.edu.cn

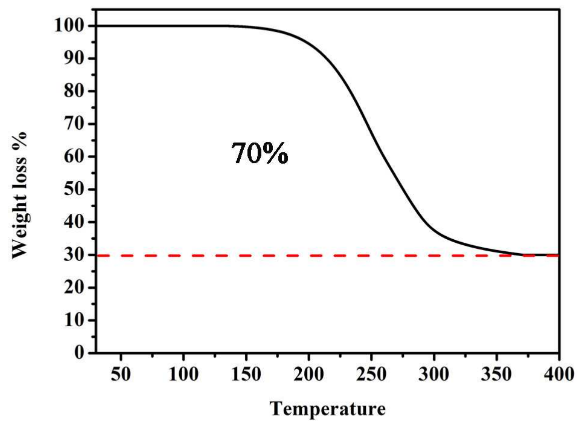

Figure S1. TGA curve of the CMK-3/S composite. The weight loss of sulfur in the CMK-3/S composite was measured to 70%.

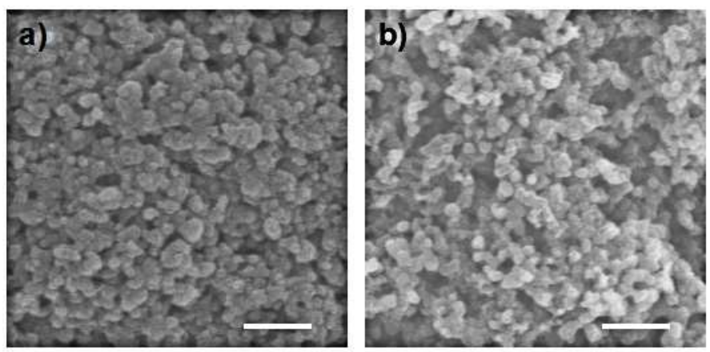

Figure S2. (a) The top surface SEM image of the PW_{12} separator and (b) SEM image of the top surface of the NENU-3 separator. Scale bar 1 µm.

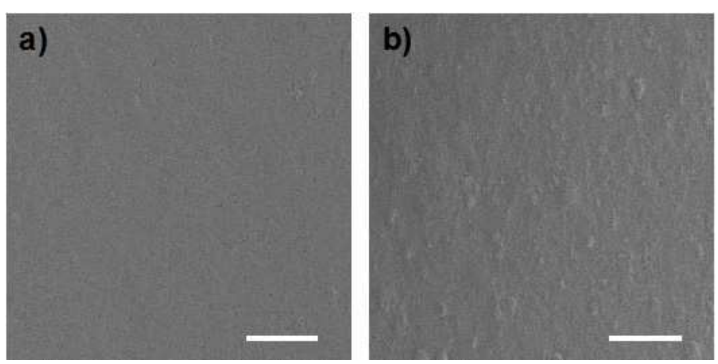

Figure S3. (a) The top surface SEM image of the PW_{12} separator and (b) SEM image of the top surface of the NENU-3 separator. Scale bar 10 µm.

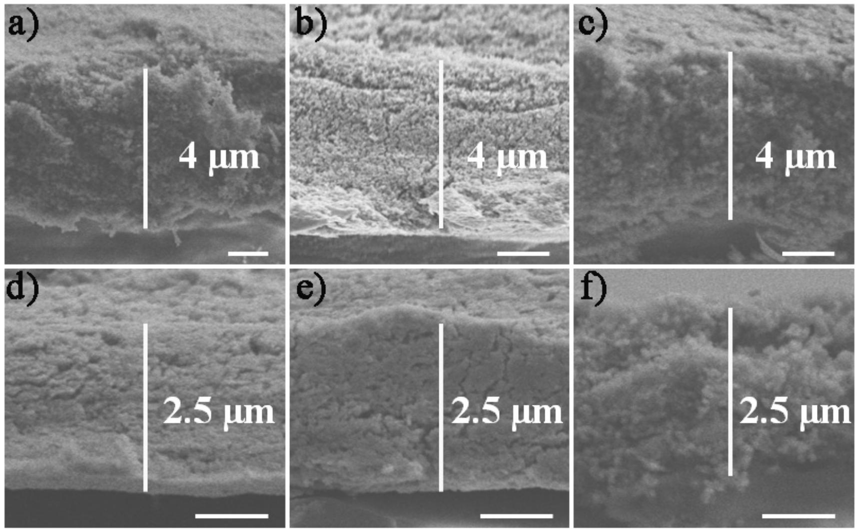

Figure S4. The cross section SEM image of the (a) PW_{12}, (b) PMo_{12}, (c) SiW_{12}, (d) NENU-3, (e) NENU-1 and (f) NENU-5 separator by coating. Scale bar 1 µm.

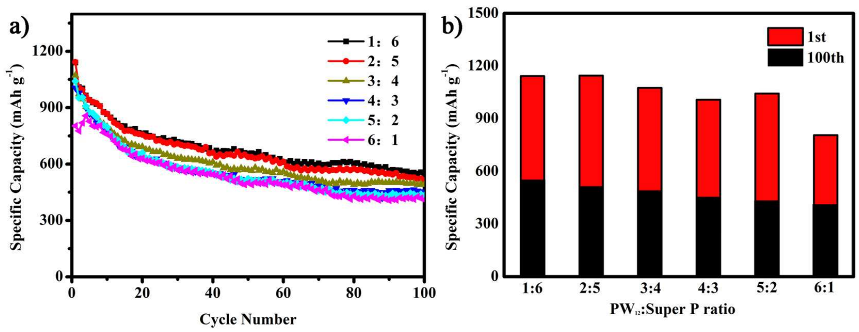

Figure S5. (a) The cycling performance comparison and (b) capacities variation of PW_{12}/Super P separator with the variation weight ratio of PW_{12} to Super P. The separator loading is 0.25 mg cm^{-2}.

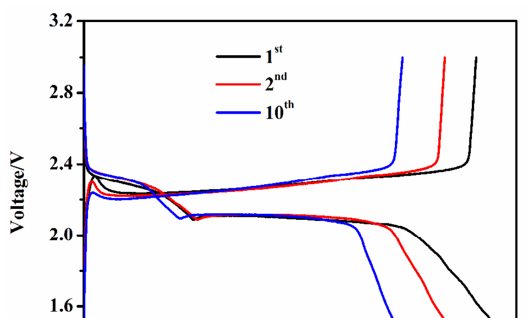

Figure S6. Typical galvanostatic charge–discharge profiles of the battery at the 1st, 2nd, and 10th cycles using PW_{12} separator when it was discharged to 1.5 V.

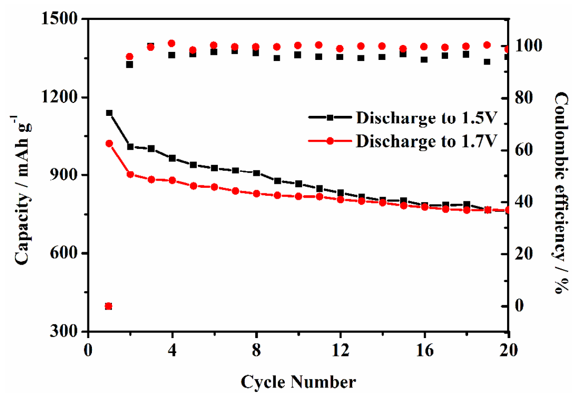

Figure S7. Comparative cycle performance of batteries using PW_{12} separator when the battery was discharged to 1.7 and 1.5 V.

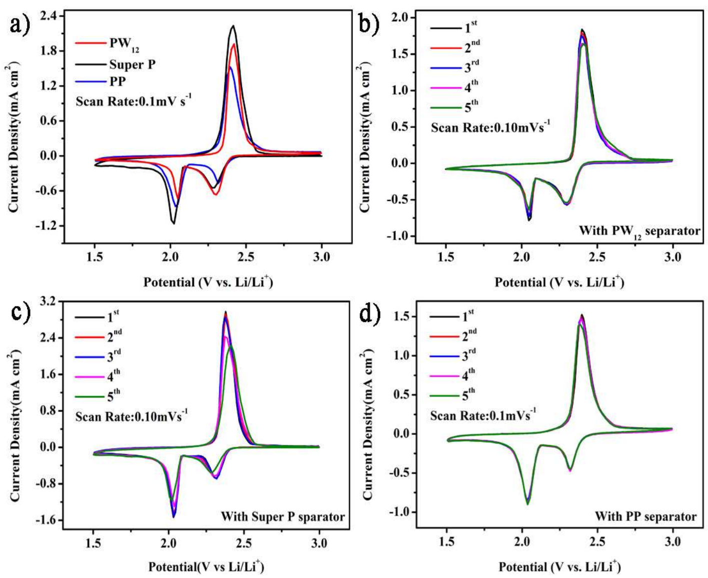

Figure S8. (a) Electrochemistry of Li-S batteries compared with PW_{12}, Super P and PP separators. Cyclic voltammetry (CV) curves of the batteries using (b) PW_{12}, (c) Super P and (d) PP separators with the 0.10 mV s^{-1}.

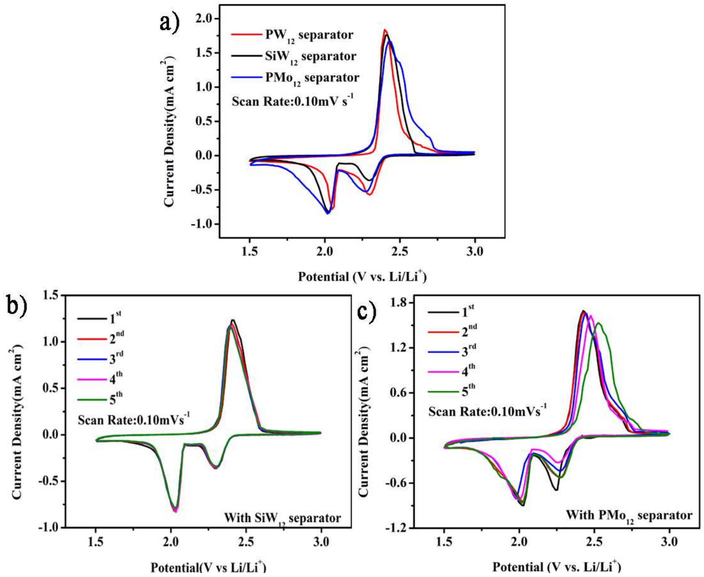

Figure S9. (a) Electrochemistry of Li-S batteries compared with PW_{12}, SiW_{12} and PMo_{12} separators. Cyclic voltammetry (CV) curves of the batteries using (b) SiW_{12} and (c) PMo_{12} separators with the 0.10 mV s^{-1}.

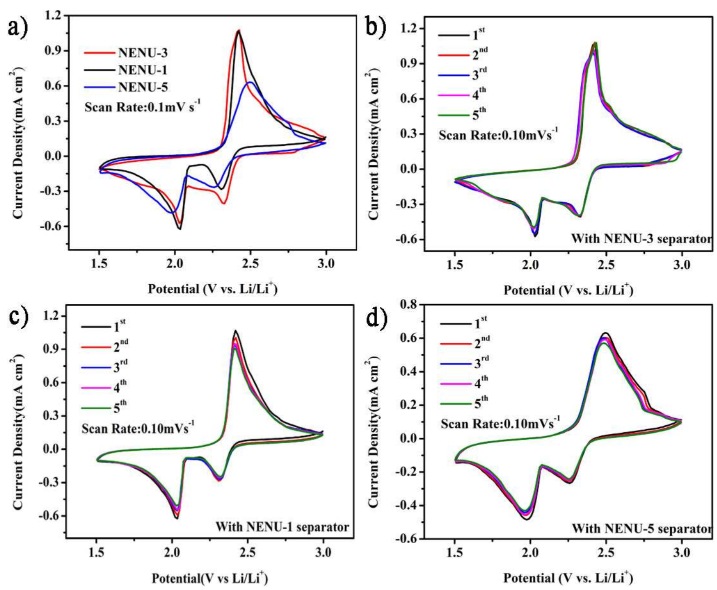

Figure S10. (a) Electrochemistry of Li-S batteries compared with PW_{12}, NENU-3, NENU-1 and NENU-5 separators. Cyclic voltammetry (CV) curves of the batteries using (b) NENU-3, (c) NENU-1 and (d) NENU-5 separators with the 0.10 mV s^{-1}.

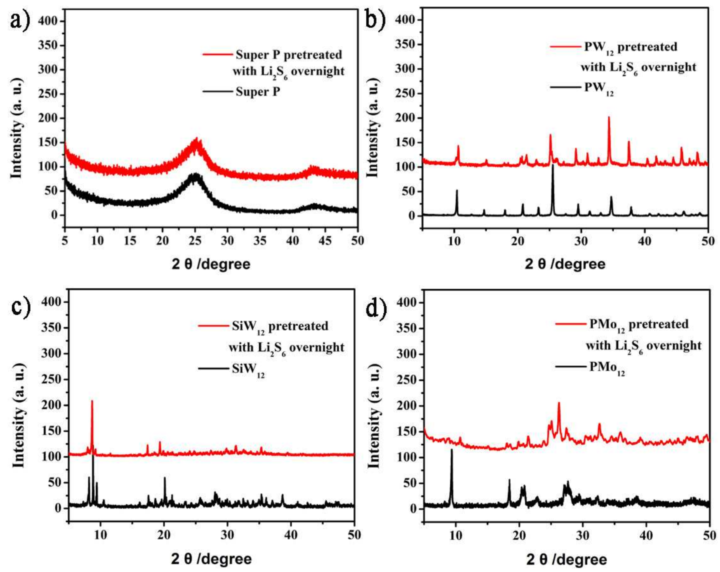

Figure S11. XRD patterns of (a) Super P, (b) PW_{12}, (c) SiW_{12} and (d) PMo_{12} pretreated with Li_2S_6 (red line) and the XRD of Super P, PW_{12}, SiW_{12} and PMo_{12} (black line).

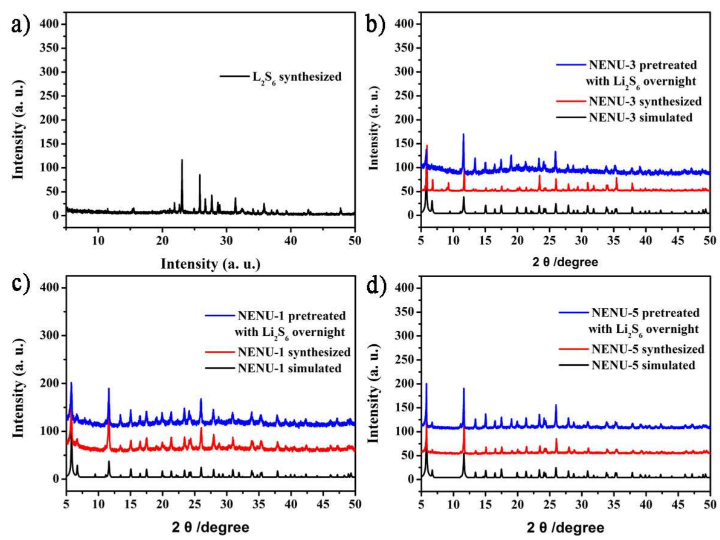

Figure S12. (a) XRD patterns of Li_2S_6 synthesized. XRD pattern of (b) NENU-3, (c) NENU-1 and (d) NENU-5 pretreated with Li_2S_6 (red line), the synthesized (blue line) and simulated XRD of NENU-3, NENU-1 and NENU-5 (black line).

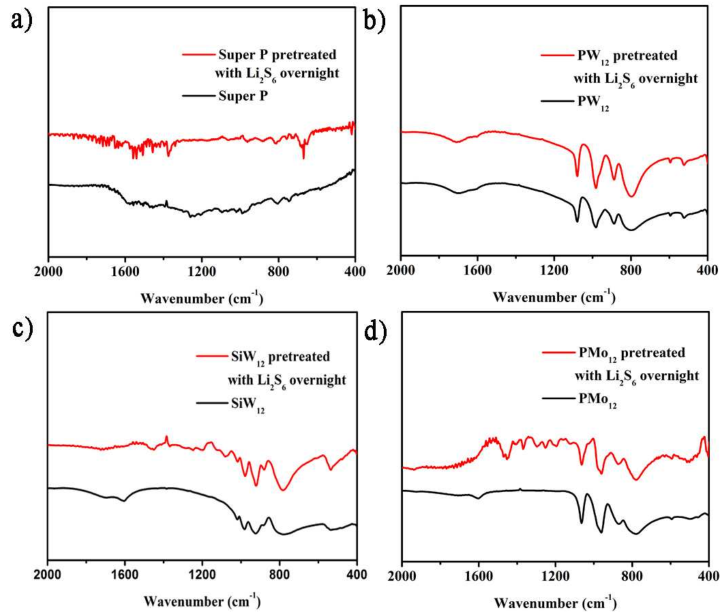

Figure S13. IR spectra of (a) Super P, (b) PW_{12}, (c) SiW_{12}, and (d) PMo_{12} pretreated with Li_2S_6 (red line) and Super P, PW_{12}, SiW_{12} and PMo_{12} (black line).

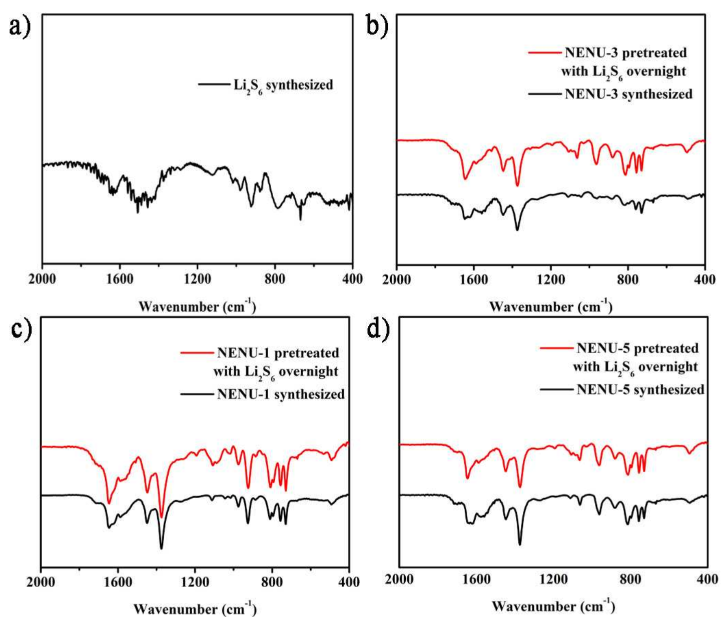

Figure S14. IR spectra of Li_2S_6 synthesized. IR spectra of (a) Li_2S_6, (b) NENU-3, (c) NENU-1 and (d) NENU-5 pretreated with Li_2S_6 (red line) and NENU-3, NENU-1 and NENU-5 synthesized (black line).

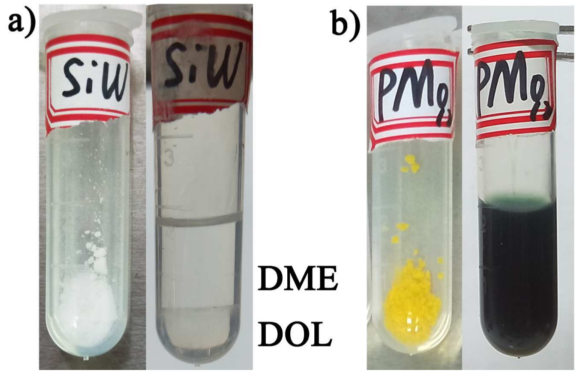

Figure S15. (a) The color change between SiW_{12} and pretreated with Li_2S_6. (b) The color change between PMo_{12} and pretreated with Li_2S_6.

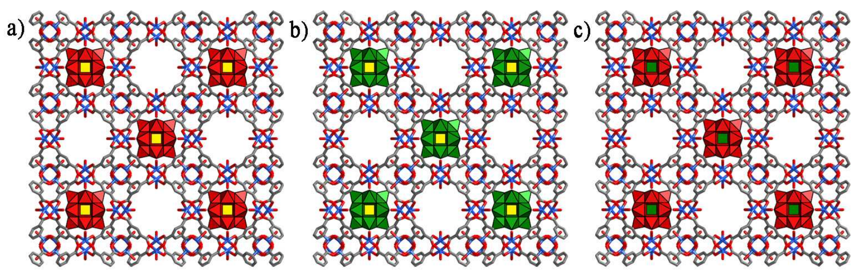

Figure S16. The structure and pore size of (a) NENU-3, (b) NENU-5 and (c) NENU-1. Grey: Carbon; Blue: Copper; Red: Oxygen.

Table S1. Physical characteristics of Super P.

	BET total surface area (m^2/g)	Particle size (nm)	Oil absorption (ml/100g)
Super P	62	40	290

Table S2. Physical characteristics of Gelgard2500 membrane.

	thickness	porosity	air permeability
Gelgard 2500	25 µm	55%	200sec/100cc

Table S3. The sulfur loading of the Li-S batteries with PP, PW_{12}, SiW_{12}, PMo_{12}, NENU-3, NENU-1 and NENU-5 separators.

separator	PP	PW_{12}	SiW_{12}	PMo_{12}
Mass loading (mg cm^{-2})	0.87	1.00	1.04	1.02
separator	NENU-3	NENU-1	NENU-5	Super P
Mass loading (mg cm^{-2})	0.89	0.91	1.01	0.98

Table S4. The Ohmic resistance of the simulated equivalent circuit of Li-S batteries with the functional separator.

Compounds	R_e (Ω)	R_f (Ω)	R_{ct} (Ω)	Sum (Ω)
PW_{12}	3.362	6.479	24.66	34.501
Fitting Error (%)	1.886	2.637	4.564	
Super P	1.809	3.693	15.72	21.222
Fitting Error (%)	9.453	6.92	6.876	
PP	6.936	32.78	57.51	97.226
Fitting Error (%)	4.365	11.77	9.813	
SiW_{12}	7.549	19.4	27.79	50.716
Fitting Error (%)	13.39	19.16	13.39	
PMo_{12}	6.781	16.78	24.79	48.351
Fitting Error (%)	3.122	2.599	6.289	
NENU-3	3.156	6.599	23.39	33.145
Fitting Error (%)	2.057	9,592	3.057	
NENU-1	2.771	8.285	23.83	34.886
Fitting Error (%)	2.703	14.59	5.356	
NENU-5	2.239	15.21	25.11	42.569
Fitting Error (%)	2.371	3.012	3.68	

Table S5. Comparisons of the electrochemical performance with serial separators in lithium-sulfur batteries

Tapy	Separator	Areal loading (mg cm^{-2})	Thickness (μm)	Sulfur/Cathode	Sulfur wt%	Mass area ratio/mg/cm^2	Cycle	Initial Capacity mAh g^{-1}	Capacity Retention mAh g^{-1}	Current density	Ref
ceramic	glass-ceramic	46	150	Sulfur/Super P	80%	1	50	800	800	0.05	1
	MMT ceramic	1.65	-	Sulfur/MWCNTs	75%	0.7	200	1382	924	100 mAh g^{-1}	2
	Celgard-AB&CNT&LAGP	-	7	Carbon/Sulfur	70%	1.5-2.0	150	1247	830	0.5C	3
Ion Conducting polymers	GO/Nafion	0.0532	0.103	carbon (graphene/CNT-hybrid)/sulfur	60%	1.2	200	1057	capacity degradation 0.18% per cycle	0.5C	4
	Nafion/interlayer	0.7-3.5	1.4-7	CNF cathode matrix and interlayer	50%	2	500	1100	500	0.2C	5
	Nafion/interlayer	0.7-3.5	1.4-7	CNF cathode matrix and interlayer	50%	2	500	1000	470	C/3	5

	Nafion/interlayer	0.7-3.5	1.4-7	CNF cathode matrix and interlayer	50%	2	500	950	450	0.5C	5
	Nafion	0.7	50	Sulfur/ Carbon Paper	50%	2	500	781	468	1.0C	6
	S-G@PP	1.3	30	Carbon/Sulfur	70%	1.5-2.1	500	-	663	3A g^{-1}	7
	S-G@PP	1.3	30	Carbon/Sulfur	70%	1.5-2.1	500	-	522	1.5A g^{-1}	7
	Super P/PP	0.2	20	Sulfur	55%	1.1-1.3	200	1400	828	0.2C	8
Carbon	Super P/Celgard	0.5	1	Super P/Sulfur	60%	1.5-2.0	500	1350	740	0.5C	9
	Mesoporous carbon	0.5	27	Super P/Sulfur	60%	1.55	500	1059	683	1C	10
	NSMPC-HS	0.5-0.6	29	CMK-3/Sulfur	71%	5.4	500	934	740	0.5C	11
graphite	AEG/CH	0.13	22.5	Super P/Sulfur	75%	1.6-2	200	992	406	0.1C	12
Cellulose	Cellulose-Based	-	30	CS_2/Sulfur	-	1.5	1000	1322	460	0.2C	13
carbon nanotube	SWCNT-Modulated	0.13	-	Super P/Sulfur	75%	1.5	300	1132	501	0.2C	14
MOFs	MOF@GO	0.3	-	CMK-3/Sulfur	70%	0.6-0.8	1500	1207	855	1C	15
	MOFs/CNTs	1.5	14	Super P/Sulfur	70%	1	300	1101	557	0.25C	16

	PW_{12}/Super P	0.25	4	CMK-3/Sulfur	70%	0.9	100	1139	-	0.1C	This Work

Reference

(1) Wang, L. N.; Zhao, Y.; Thomas, M. l.; Dutta, A.; Byon, H. R. Sulfur-Based Catholyte Solution with a Glass-Ceramic Membrane for Li–S Batteries. *ChemElectroChem.* **2016,** *3,* 152–157.

(2) Ahn, W., Lim, S. N. Lee, D. U., Kim, K. B., Chen, Z. W., Yeon, S. H. Interaction mechanism between a functionalized protective layer and dissolved polysulfide for extended cycle life of lithium sulfur batteries. *J. Mater. Chem.* A. **2015,** *3,* 9461.

(3) Wang, Q. S.; Wen, Z. Y.; Yang, J. H.; Jin, J.; Huang, X.; Wu, X, W.; Han, J. D. Electronic and ionic co-conductive coating on the separator towards high-performance lithiumesulfur batteries. *Journal of Power Sources.* **2016,** *306,* 347-353.

(4) Zhuang, T. Z.; Huang, J. Q.; Peng, H. J.; He, L. Y.; Cheng, X. B.; Chen, C. M.; Zhang, Q. Rational Integration of Polypropylene/Graphene Oxide/Nafion as Ternary-Layered Separator to Retard the Shuttle of Polysulfides for Lithium–Sulfur Batteries. *Small.* **2016,** *12,* 381–389.

(5) Huang, J. Q.; Zhang, Q.; Peng, H. J.; Liu, X. Y.; Qian, W. Z.; Wei, F. Ionic shield for polysulfides towards highly-stable lithium–sulfur batteries. *Energy Environ. Sci.* **2014,** *7,* 347–353.

(6) Yu, X. W.; Joseph, J.; Manthiram, A. Polymer lithium–sulfur batteries with a Nafion membrane and an advanced sulfur electrode. *J. Mater. Chem. A.* **2015,** *3,* 15683.

(7) Zhou, C. M.; Li, L.; Wang, D. W.; Shan, X. Y.; Pei, S. F.; Li, F.; Cheng, H. M. A Flexible Sulfur-Graphene-Polypropylene Separator Integrated Electrode for Advanced Li-S Batteries. *Adv. Mater.* **2015,** *27,* 641-647.

(8) Chung, S. H.; Manthiram, A. Bifunctional Separator with a Light-Weight Carbon-Coating for Dynamically and Statically Stable Lithium-Sulfur Batteries. *Adv. Funct. Mater.* **2014,** *24,* 5299–5306.

(9) Yao, H. B.; Yan, K.; Li, W. Y.; Zheng, G. Y.; Kong, D. S.; She, Z. W.; Narasimhan, V. K.; Liang, K.; Cui, Y. Improved lithium–sulfur batteries with a conductive coating on the separator to prevent the accumulation of inactive S-related species at the cathode–separator interface. *Energy Environ. Sci.* **2014,** *7,* 3381.

(10) Balach, J.; Jaumann, T.; Klose, M.; Oswald, S.; Eckert, J.; Giebeler, L. Functional Mesoporous Carbon-Coated Separator for Long-Life, High-Energy Lithium–Sulfur Batteries. *Adv. Funct. Mater.* **2015.** *25,* 5285−5291.

(11) Balach, J.; Singh, H.K.; Gomoll, S.; Jaumann, T.; Klose, M.; Oswald, S.; Richter, M.; Eckert, J.; Giebeler, L. Synergistically Enhanced Polysulfide Chemisorption Using a Flexible Hybrid Separator with N and S Dual-Doped Mesoporous Carbon Coating for Advanced Lithium−Sulfur Batteries. *Acs Applied Materials & Interfaces.* **2016,** *8,* 14586−14595.

(12) Abbas, S. A.; Ding, J.; Wu, S. H.; Fang, J.; Boopathi, K. M.; Mohapatra, A.; i Lee, L. W.; Wang, P. C.; Chang, C. C.; Chu, C. W. Modified Separator Performing Dual Physical/Chemical Roles

to Inhibit Polysulfide Shuttle Resulting in Ultra-Stable Li–S Batteries. *ACS Nano.* **2017,** *11,* 12436–12445.

(13) Yu, B. C.; Park, K.; Jang, J. H.; Goodenough, J. B. Cellulose-Based Porous Membrane for Suppressing Li Dendrite Formation in Lithium−Sulfur Battery. *ACS Energy Lett.* **2016,** *1,* 633−637.

(14) Chang, C. H.; Chung, S. H.; Manthiram, A. Effective Stabilization of a High-Loading Sulfur Cathode and a Lithium-Metal Anode in Li-S Batteries Utilizing SWCNT-Modulated Separators. *Small.* **2016,** *12,* No. 2, 174–179.

(15) Bai, S.; Liu, X. J.; Zhu, K.; Wu, S.; Zhou, H. Metal–organic framework-based separator for lithium–sulfur batteries. *Nat. Energy.* **2016,** *1.* 16094.

(16) Li, M. L.; Wan, Y. Huang, J. K.; Assen, A. H.; Hsiung, C. E.; Jiang, H.; Han, Y.; Eddaoudi, M.; Lai, Z. P.; Ming, J.; Li, L. J. Metal−Organic Framework-Based Separators for Enhancing Li−S Battery Stability: Mechanism of Mitigating Polysulfide Diffusion. *ACS Energy Lett.* **2017,** *2,* 2362−2367.